Vacancy motion in rare-earth-deficient $R_{1-x}Ni_2$ Laves phases observed by perturbed angular correlation spectroscopy

M. Forker,* P. de La Presa, and S. Müller
Helmholtz-Institut für Strahlen- und Kernphysik, Nussallee 14-16, D-53115 Bonn, Germany

A. Lindbaum and E. Gratz
Institut für Festkörperphysik, Vienna University of Technology, Wiedner Hauptstr. 8-10, A-1040 Vienna, Austria
(Received 2 December 2003; revised manuscript received 21 April 2004; published 19 July 2004)

Rare-earth-deficient $R_{1-x}Ni_2$ Laves phases, which reportedly crystallize in a $C15$ superstructure with ordered R vacancies, have been investigated by perturbed angular correlation (PAC) measurements of electric quadrupole interactions at the site of the probe nucleus ^{111}Cd. Although ^{111}Cd resides on the cubic R site, a strong axially symmetric quadrupole interaction (QI) with frequencies $\nu_q \approx 265-275$ MHz has been found in the paramagnetic phases of $R_{1-x}Ni_2$ with $R=$Pr, Nd, Sm, Gd. This interaction is not observed for the heavy R constituents $R=$Tb, Dy, Ho, Er. The fraction of probe nuclei subject to the QI in $R_{1-x}Ni_2$, $R=$Pr, Nd, Sm, Gd, decreases from 100% at low temperatures to zero at $T>300$ K and 500 K for $R=$Sm, Gd and $R=$Pr, Nd, respectively. At $T=100$ K the QI is static within the PAC time window, but at $T=200$ K fluctuations with correlation times $\tau_C < 10^{-6}$ s, have been detected. These observations can be explained consistently by two assumptions: (i) the mother isotope ^{111}In of the PAC probe ^{111}Cd constitutes an attractive potential for vacancies and (ii) the R vacancies in $R_{1-x}Ni_2$ are highly mobile at temperatures $T<300$ K, which is incompatible with a static vacancy superstructure. The measurements indicate a decrease of the vacancy-probe binding energy from the light to the heavy R constituents of $R_{1-x}Ni_2$. For $R=$Pr, Nd, Sm, Gd the binding energy is in the range 0.15–0.40 eV. The activation energy E_A for vacancy jumps near the probe derived from the temperature dependence of the nuclear spin relaxation at 200 K $\leqslant T \leqslant$ 300 K is small. The values observed in different samples cover a range of 0.1 eV $\leqslant E_A \leqslant$ 0.23 eV. The trial frequency w_0 of these jumps appears to be correlated to the activation energy: $\ln w_0(\mathrm{MHz}) \approx 58 E_A(\mathrm{eV})$. At high temperatures $T>500$ K nuclear spin relaxation related to vacancy hopping is observed in nearly all $R_{1-x}Ni_2$. Auxiliary ^{111}Cd PAC measurements have been carried in $Sc_{0.95}Ni_2$, $ScNi_2$, $ScNi_{0.97}$, Gd_2Ni_{17}, $GdNi_5$, $GdNi_3$, and GdNi.

DOI: 10.1103/PhysRevB.70.014302 PACS number(s): 76.60.Es, 61.72.Ji, 76.80.+y

I. INTRODUCTION

We have recently used the perturbed angular correlation (PAC) technique for an investigation of the magnetic hyperfine interaction in the $C15$ rare earth (R) Laves phases RCo_2 (Refs. 1 and 2) with particular emphasis on the rare-earth dependence of the saturation field at low temperatures and on the order of the magnetic phase transitions. To disentangle the contributions of the itinerant $3d$ electrons of Co and the highly localized $4f$ electrons of the rare earths to the magnetic hyperfine interaction, an extension of these studies to RNi_2 appeared of interest, because in contrast to RCo_2, RNi_2 shows no $3d$ moments and the magnetic order is determined by the indirect $4f$-$4f$ interaction alone.[3]

In the paramagnetic phase of RCo_2 the angular correlation was found to be unperturbed, indicating that the PAC probe nucleus ^{111}Cd employed in this study resides on the cubic R site. On the noncubic Co site the probe nucleus would experience a perturbation by a strong electric quadrupole interaction (QI). One would expect that in RNi_2 ^{111}Cd also occupies the R site and measurements[4] carried out with $GdNi_2$ ($T_C=75$ K) and $SmNi_2$ ($T_C=23$ K) showed in fact an unperturbed angular correlation at elevated temperatures ($T \geqslant 600$ K) of the paramagnetic phase. Upon cooling, however, we observed a strong axially symmetric QI in paramagnetic $GdNi_2$, which apparently is fluctuating at intermediate temperatures and becomes static at temperatures $T \leqslant 200$ K.

To elucidate the origin of this unexpected QI, a systematic ^{111}Cd PAC investigation of the hyperfine interactions in paramagnetic RNi_2 was carried out. The results of this study, which strongly suggest that the QI is related to the diffusion of vacancies in RNi_2, are presented in this paper.

According to recent experimental data[5–9] and theoretical studies,[10] RNi_2 does not crystallize in the pure cubic $C15$ structure, observed, e.g., in RCo_2. Single phase compounds can only be obtained for rare-earth-deficient $R_{1-x}Ni_2$. The x-ray diffraction patterns of these compounds are explained by a $C15$ superstructure (space group $F\bar{4}3m$) in which the $4a$ sites of the R sublattice are only partially occupied. The occupancy N of site $4a$ increases from the light R to the heavy R constituents. In $Pr_{1-x}Ni_2$ one has $N \approx 0.1$, corresponding to $x=0.056$, and in $LuNi_2$ ($N=1$, $x=0$) the superstructure is not observed. As the temperature is increased, the superstructure lines disappear from the x-ray diffraction spectra. This reversible order-disorder transition, which can also be induced by the application of pressure,[9] occurs at temperatures $T>400$ K (Refs. 7 and 9). The instability of the $C15$ structure in the case of $R_{1-x}Ni_2$ is usually attributed to the fact that the atomic radius radio r_R/r_{Ni} is much larger than that of the most compact $C15$ arrangement of hard spheres. In these space filling arguments, the stress resulting

from the mismatch of the atomic volumes is released by the introduction of R vacancies.

II. EXPERIMENTAL DETAILS

A. Sample preparation and equipment

The PAC measurements were carried out mainly with the 171–245 keV cascade of ^{111}Cd, which is populated by the electron capture decay of the 2.8 d isotope ^{111}In. The intermediate state of the cascade has a half-life of $t_{1/2}=84$ ns, and its spin is $I=5/2$. The samples were doped with the PAC probe ^{111}Cd by diffusion (800 °C, 12 h) of radioactive ^{111}In into the host lattice. From the γ-ray intensity of the samples we estimate the ^{111}In concentration to be $\geqslant 10^{-8}$. In one case, we used the β decay of the 7.5 d isotope ^{111}Ag to populate the 245 keV state of ^{111}Cd. For this purpose, radioactive ^{111}Ag was implanted into $GdNi_2$ with an energy of 160 keV.

The compounds were prepared by arc melting of the metallic components in an argon atmosphere. Samples of RNi_2 with the stoichiometry ratio 1:2 were produced for the rare-earth constituents R=Pr, Nd, Sm, Gd, Tb, Dy, Ho, Er, and Y. Furthermore, $Gd_{0.95}Ni_2$ and $Gd_{1.05}Ni_2$ were investigated. To exclude that a low-temperature structural change is responsible for the QI observed below 200 K, x-ray diffraction measurements were carried out on $GdNi_2$ and $SmNi_2$ at 290 K and 50 K. Single-phase $C15$ diffraction patterns were observed at both temperatures, with the lattice parameter a decreasing by about 1% from 290 K to 50 K. For all other compounds the absence of foreign phases was established by x-ray diffraction measurements at room temperature. In addition to the RNi_2 samples prepared in the course of this study, measurements were also carried with the single-phase compounds $Sm_{0.95}Ni_2$, $GdNi_2$, $Tb_{0.98}Ni_2$, and $Y_{0.95}Ni_2$, which have been previously studied and characterized by resistivity, thermal expansion, and x-ray diffraction measurements.[7]

The influence of the indium concentration on the fraction of probe nuclei subject to an axially symmetric QI was investigated by adding stable indium with concentrations of 1 and 3 at.% to samples of $SmNi_2$ and $PrNi_2$.

$ScNi_2$ can be considered as an "ideal" Laves phase. The ratio of the atomic radii $r_{Sc}/r_{Ni}=1.225$ corresponds to that of the most compact $C15$ arrangement of hard spheres and $ScNi_2$ crystallizes in the $C15$ structure without showing any superstructure lines. Furthermore, contaminations by impurity phases are not expected because of the large homogeneity range of $ScNi_2$. For a comparison of the PAC spectra observed in $R_{1-x}Ni_2$ with that of an ideal Laves phase the investigation of $ScNi_2$ therefore appeared of interest. In addition, the effect of disordered vacancies in the R and Ni sublattices of a Laves phase was studied by extending the measurements to $Sc_{0.95}Ni_2$ and $ScNi_{1.97}$. X-ray diffraction measurements showed that all Sc-Ni compounds were single phase with lattice parameters $a=0.6917$, 0.6926, 0.6929 nm for $Sc_{0.95}Ni_2$, $ScNi_2$, and $ScNi_{1.97}$, respectively.

To exclude the possibility that the QI observed in ^{111}Cd:RNi_2 results from a contamination by an impurity phase, the ^{111}Cd QI was also determined in Gd_2Ni_{17}, $GdNi_5$, $GdNi_3$, and GdNi, the other intermetallic compounds of the Gd-Ni system. The PAC measurements were carried out with a standard four-detector BaF_2 setup in the temperature range $10\ \text{K} \leqslant T \leqslant 1273\ \text{K}$. Temperatures $T<290$ K were obtained with a closed-cycle He refrigerator; temperatures $T>290$ K were produced with an especially designed PAC furnace.[11] For the high-temperature measurements, the samples were encapsulated into small quartz tubes.

The order-disorder transition of $Sm_{0.95}Ni_2$—one of the samples showing a QI at low temperatures—was investigated by x-ray diffraction in the range $100\ \text{K} \leqslant T \leqslant 440\ \text{K}$. In this experiment, which used a Siemens diffractometer equipped with a He-flow cryostat, the intensity of the superstructure lines (422), (511), (531), and (442) was measured as a function of temperature.

B. Data analysis

The angular correlation theory of two successive γ rays of a γ-γ cascade, expressed by angular correlation coefficients A_{kk} ($k=2,4$) may be modulated in time by hyperfine interactions in the intermediate state of the cascade. For polycrystalline samples this modulation can be described by the perturbation factor $G_{kk}(t)$, which depends on the multipole order, the symmetry, and time dependence of the interaction and on the spin of the intermediate state (for details see, e.g., Frauenfelder and Steffen[12]).

In this paper we are dealing with perturbations by the hyperfine interaction between the electric quadrupole moment Q of the intermediate state and an electric field gradient (EFG) acting at the nuclear site. The electric quadrupole interaction can be completely described by two independent parameters, the quadrupole frequency $\nu_q=eQV_{zz}/h$ and the asymmetry parameter $\eta=(V_{xx}-V_{yy})/V_{zz}$, where $V_{ii}=\partial^2 V/\partial i^2$ ($i=x,y,z$) are the principal-axis components of the EFG tensor with $|V_{xx}|\leqslant|V_{yy}|\leqslant|V_{zz}|$. Both static and time-dependent EFG's were observed in this investigation.

In the case of a static electric quadrupole interaction the perturbation factor has the general form:

$$G_{kk}(t;\nu_q,\eta,\delta)=s_{k0}+\sum_n s_{kn}\cos(\omega_n,t)\exp(-1/2\,\delta\omega_n t). \tag{1}$$

The hyperfine frequencies ω_n are the frequencies associated with the energy differences between the hyperfine levels into which the nuclear state is split by the QI. These frequencies depend on the quadrupole frequency $\nu_q=eQV_{zz}/h$ and the asymmetry parameter η. In polycrystalline samples the amplitudes s_{kn} are functions of η only. The number n of terms in Eq. (1) depends on the spin of the nuclear state under consideration. For $I=5/2$ one has $n=3$. The exponential factor accounts for possible distributions of the static QI caused by structural or chemical defects, which lead to an attenuation of the oscillatory PAC pattern. The parameter δ is the relative width of a Lorentzian distribution.

Frequently, several fractions of nuclei subject to different hyperfine interactions (HFI's) are found in the same sample. The effective perturbation factor is then given by

$$G_{kk}(t) = \sum_i f_i G^i_{kk}(t). \quad (2)$$

f_i (with $\Sigma_i f_i = 1$) is the relative intensity of the ith fraction.

In the case of time-dependent EFG's, the fluctuating QI's induce transitions between the hyperfine levels of the intermediate state. The effect of the resulting nuclear spin relaxation on the angular correlation depends on the fluctuation rate w. Slow fluctuations ($w \ll \nu_q^0$; ν_q^0 is the center of the static distribution of quadrupole frequencies) lead to an attenuation of the angular correlation that becomes observable when the correlation time τ_C of the fluctuation is of the same order of magnitude as the PAC time window ($\sim 10\tau_N$; τ_N is the lifetime of the nuclear state). With increasing fluctuation rate w the nuclear spin relaxation increases. The resulting attenuation of the angular correlation first increases towards a maximum at $w \approx \nu_q^0$ and then—in the fast-fluctuation region with $w > \nu_q^0$—decreases again, analogous to the motional narrowing of a NMR signal. Qualitatively, the PAC signature of a dynamic process therefore is a temperature-dependent, reversible attenuation of the angular correlation, which passes through a maximum as one moves from the slow to the fast-fluctuation regime.

Time-dependent QI's in solids are in most cases the result of atomic motion. The effect of the nuclear spin relaxation caused by jumping atoms on the angular correlation is most appropriately described by Blume's stochastic theory,[13,14] which, however, is very difficult to apply if the motion leads not only to fluctuations of the orientation, but also of the strength and symmetry of the EFG tensor. The analysis of experimental data is therefore frequently based on an approximation of the Blume theory with a single relaxation parameter λ_k:

$$G_{kk}(t) = \Gamma_{kk}(t)\exp(-\lambda_k t). \quad (3)$$

The validity of this approximation is discussed in Refs. 15 and 16. For slow fluctuations ($w \ll \nu_q^0$) the function $\Gamma_{kk}(t)$ is given by the perturbation factor of a static distribution of HFI's [Eq. (1)] and the relaxation parameter is $\lambda_k = \alpha w$, where w is the hopping rate and α is determined by the ratio of the fluctuating to the static interaction ($\alpha = 1$ in the absence of a static interaction). In the case of overbarrier diffusion with an Arrhenius relation of the jump rate $w = w_0 \exp(-E_A/kT)$ (E_A is the activation energy) and slow fluctuations, the relaxation parameter therefore increases with increasing temperature according to $\lambda_k = \lambda_k^0 \exp(-E_A/kT)$.

Fast fluctuations are adequately described by Eq. (3) if several jumps occur within one spin precession period ($w \geq 5\nu_q^0$). In the fast-fluctuation regime the function $\Gamma_{kk}(t)$ is determined by the time average of the interaction. In the case of a vanishing time average one has $\Gamma_{kk}(t) = 1$. The relaxation parameter λ_k corresponds to the Abragam and Pound spin relaxation constant,[17] which for the case of a fluctuating QI of strength ν_q^f, correlation time $\tau_C = 1/w$ (τ_C is the residence time between jumps), and nuclear spin I is given by

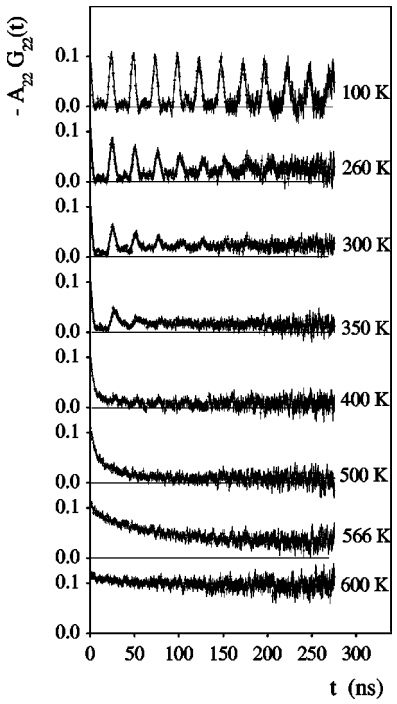

FIG. 1. PAC spectra of ^{111}Cd in $PrNi_2$ between 100 K and 600 K.

$$\lambda_k = (3\pi^2/5)\tau_C(\nu_q^f)^2 k(k+1)\frac{4I(I+1) - k(k+1) - 1}{[2I(2I-1)]^2}. \quad (4)$$

In the fast-fluctuation regime the relaxation parameter therefore decreases with increasing temperature according to $\lambda_k = \lambda_k^0 \exp(E_A/kT)$.

III. MEASUREMENTS AND RESULTS

The ^{111}In/^{111}Cd PAC spectra observed in the paramagnetic phase at low temperatures divide the RNi$_2$ series into two groups. (Note: For simplicity, the notation "RNi$_2$" shall be used in the following for all compounds investigated.) In the first group consisting of R=Pr, Nd, Sm, and Gd (in the following termed "light RNi$_2$") the ^{111}Cd angular correlation is perturbed by a strong axially symmetric QI. In the second group with the heavy R=Tb, Dy, Ho, and Er (" heavy RNi$_2$") this quadrupole perturbation is not observed. YNi$_2$ is on the border of these two groups, with some samples showing a small fraction of probe nuclei subject to the QI. In the following the details and main results of these measurements shall be described.

A. Light RNi$_2$: R=Pr, Nd, Sm, Gd, and Y

For an illustration of the typical perturbations in the light RNi$_2$, we show in Figs. 1 and 2 the evolution of the PAC spectra of ^{111}In/^{111}Cd in $PrNi_2$ and $GdNi_2$, respectively, from 100 K to 600 K. Three temperature ranges with pronounced differences in the spectra can be recognized.

(i) At $T_C < T \leq 150$ K one observes in all light RNi$_2$ a periodic, almost nonattenuated modulation of the anisotropy with time, which is typical for a perturbation by a unique

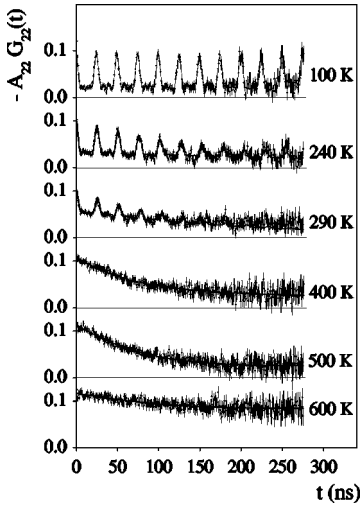

FIG. 2. PAC spectra of ^{111}Cd in $GdNi_2$ between 100 K and 600 K.

axially symmetric QI. Most low-temperature spectra consist of only one component or fraction, with all probe nuclei subject to the same QI (in the following termed as "QI-modulated fraction"). In the samples of $GdNi_2$ doped with ^{111}Cd by implantation of ^{111}Ag this QI was not detected. After annealing the sample at 1000 K to remove eventual radiation damage, the ^{111}Ag/^{111}Cd PAC was found to be unperturbed.

(ii) At intermediate temperatures $T>200$ K a second, only weakly perturbed component appears (in the following termed as "cubic" component for reasons discussed below). This second component is clearly visible in Fig. 2 as a shift of the baseline of the periodic modulation (see the spectrum at 290 K). As temperature increases, the cubic fraction grows at the expense of the QI-modulated fraction. For $NdNi_2$ and $PrNi_2$ the temperature dependence of the cubic fraction is much weaker than that for $GdNi_2$ and $SmNi_2$. This is obvious from the $PrNi_2$ spectra in Fig. 1 where the baseline of the periodic modulation barely shifts with increasing temperature.

The second remarkable feature of the spectra in the intermediate temperature range is the decay of the oscillation amplitudes with time, which sets in simultaneously with the appearance of the cubic component. This attenuation, which increases reversibly with temperature, reflects a nuclear spin relaxation and indicates that relative to the PAC time window the perturbing QI has become time-dependent. Up to $T=400$ K the periodic modulation is completely wiped out in all light RNi_2.

The observation of two components leads to a two-fraction model for the numerical analysis in the range $100\ \mathrm{K}\leqslant T\leqslant 400$ K:

$$G_{22}(t) = fG_{22}^{I}(t) + (1-f)G_{22}^{II}(t). \qquad (5)$$

Here f denotes the fraction of probe nuclei subject to the QI, and $(1-f)$ the cubic fraction. To allow for a dynamic perturbation of the QI-modulated fraction, the perturbation factor $G_{22}^{I}(t)$ was assumed to have the form of Eq. (3) with the relaxation parameter λ_2 describing the attenuation by nuclear spin relaxation and $\Gamma_{22}(t)$ given by the static perturbation function of Eq. (1).

TABLE I. The quadrupole frequency ν_q(100 K) of ^{111}Cd on the R site of RNi_2 for $R=$Pr, Nd, Sm, Gd and the temperature $T(f_0/2)$ at which the fractions of ^{111}Cd nuclei decorated with a vacancy has dropped to 50%. The values of $T(f_0/2)$ obtained for different samples of the same compound vary up to 20%.

RNi_2	ν_q(MHz) at 100 K	$T(f_0/2)$ (K)
$PrNi_2$	272.9(5)	550–750
$NdNi_2$	270.7(5)	440–450
$SmNi_2$	266.7(5)	280–350
$GdNi_2$	267.5(5)	250–300
YNi_2	258.4(5)	
$Sm_{0.99}In_{0.01}Ni_2$	264.7(5)	350
$Sm_{0.97}In_{0.03}Ni_2$	264.9(5)	>500

The periodicity of the PAC pattern at 100 K clearly shows that the perturbing QI has axial symmetry. The asymmetry parameter of the QI-modulated fraction was therefore fixed in the analysis to $\eta=0$. The Lorentzian distribution of the QI was assumed to be temperature independent and its width fixed to the low-temperature value of $\delta\approx 0.01$. The weak interaction responsible for the slow decrease of the anisotropy of the cubic component (G_{22}^{II}) was assumed to be static. With Eq. (1) this component can be reproduced by a distribution of QI's centered at $\nu_q\approx 2-3$ MHz.

The parameters of main interest are the quadrupole frequency ν_q, the relative amplitude f, and the relaxation parameter λ_2 of the QI-modulated fraction. The quadrupole frequency at 100 K is listed in Table I. The temperature dependence of ν_q is weak, $\partial\ln\nu_q/\partial T\approx -1.5\times 10^{-4}$ K^{-1} is almost an order of magnitude smaller than the value found with ^{111}Cd, e.g., in the R metals.[18]

Figure 3 shows the typical temperature dependence of the QI-modulated fraction. Figure 4 is an Arrhenius plot of the relaxation parameter λ_2 of the group of the light RNi_2 in the

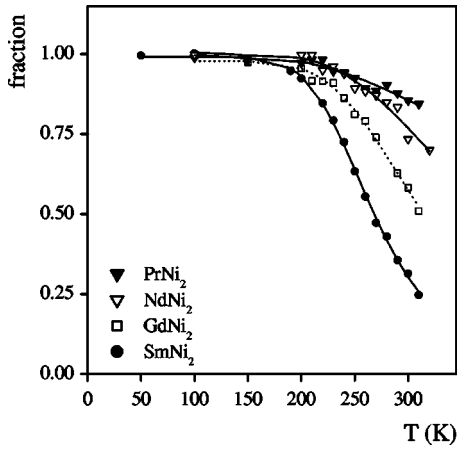

FIG. 3. The temperature dependence of the fraction of ^{111}Cd probe nuclei in RNi_2 with $R=$Pr, Nd, Sm, Gd subject to an axially symmetric QI with frequency $\nu_q=260-270$ MHz.

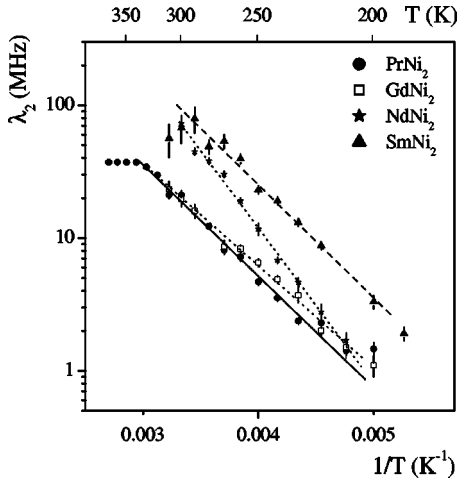

FIG. 4. Arrhenius plot of the relaxation parameter λ_2 describing the attenuation of the periodic modulation of the spectra of ^{111}Cd:RNi$_2$ between 200 K and 300 K.

intermediate temperature range 200 K$\leqslant T\leqslant$400 K.

At this point it is very interesting to compare these PAC results to the x-ray diffraction measurements on $Sm_{0.95}Ni_2$ carried out in the temperature range 100 K$\leqslant T\leqslant$440 K. In Fig. 5 the intensity of the superstructure lines (422), (511), (531), and (442), normalized to the intensity of the (440) and (622) reflections of the cubic Laves phase, is shown as a function of temperature. The superstructure intensity starts to appear at $T\approx$450 K and saturates at ~350 K, giving the impression that a stable vacancy structure has been reached at this temperature. The PAC spectra, however, give clear evidence for atomic motion leading to nuclear relaxation at temperatures well below T=350 K.

The relaxation parameter λ_2 follows the Arrhenius relation $\lambda_2=\lambda_2^0\exp(-E_A/k_BT)$, indicating that the spin depolarization at $T<$300 K is caused by a slowly fluctuating interaction (see Sec. II B). The activation energies E_A derived from the experimental $\lambda_2(T)$ values extend over the range 0.1 eV $\leqslant E_A\leqslant$0.23 eV (see Fig. 6). The highest values were found in NdNi$_2$, the smallest in $Sm_{1-x}In_xNi_2$ with x=0.1 and 0.03.

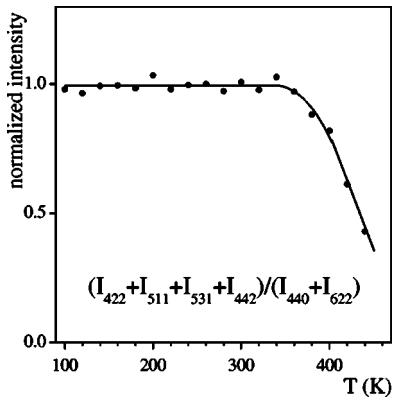

FIG. 5. The temperature dependence of the intensity of the superstructure lines (422), (511), (531), and (442) in the x-ray diffraction spectrum of $Sm_{0.95}Ni_2$ compared to the intensity of the (440) and (622) reflections of the cubic Laves phase.

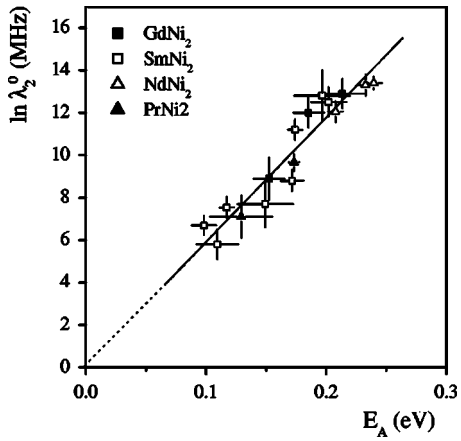

FIG. 6. The preexponential factor λ_2^0 of the Arrhenius relation $\lambda_2=\lambda_2^0\exp(-E_A/k_BT)$ vs the activation energy E_A of different compounds RNi$_2$.

The range ΔE_A of activation energies observed in different samples of the same compound is relatively small for PrNi$_2$ and NdNi$_2$ ($\Delta E_A\leqslant$0.03 eV), but quite large for GdNi$_2$ ($\Delta E_A\leqslant$0.06 eV) and SmNi$_2$ ($\Delta E_A\leqslant$0.1 eV). A correlation between the different E_A values of the same compound and sample preparation parameters (e.g., annealing) or the stoichiometry ratio could not be detected.

The preexponential factor λ_2^0 of the Arrhenius relation $\lambda_2=\lambda_2^0\exp(-E_A/k_BT)$ fitted to the experimental data of $\lambda_2(T)$ was found to vary over several orders of magnitude. This variation is manifest in Fig. 4 where the relaxation parameter λ_2 at a given temperature (e.g., 250 K) in compounds RNi$_2$ with quite similar E_A values differs up to factor of 10.

In Fig. 6 we have collected the preexponential factors λ_2^0 and the activation energies E_A for all investigated compounds. The plot shows a clear linear relation between ln λ_2^0 and the activation energy E_A. The solid line in Fig. 6 corresponds to ln $\lambda_2^0=0.0(7)+58(4)E_A$.

(iii) Between $T\approx$400 K and 600 K one observes a recovery of the angular correlation from a perturbed to an unperturbed pattern. At 400 K the anisotropy decreases monotonically to zero in all light RNi$_2$; in PrNi$_2$ (Fig. 1) and NdNi$_2$, however, this decrease is much faster than in GdNi$_2$ (Fig. 2) and SmNi$_2$. A fast monotonic decrease of the anisotropy with time may be caused either by a broad distribution of strong static interactions or by a fluctuating interaction. Strong attenuations by a dynamic QI occur when $\nu_q^f\tau_C\approx 1$, where ν_q^f characterizes the strength of the fluctuating interaction and τ_C its correlation time. The two possibilities may be distinguished by the anisotropy at large delay times: While a fluctuating interaction with $\nu_q^f\tau_C\approx 1$ completely destroys the anisotropy, a distribution of static interactions leads to a constant ("hard core") value of $G_{22}(t)=0.2$ at large delay times. The complete attenuation of the anisotropy to zero in PrNi$_2$ and NdNi$_2$ at 400 K is therefore clear evidence for a perturbation by a rapidly fluctuating interaction. As temperature is raised beyond 400 K, the anisotropy is increasingly restored and at T=600 K the angular correlation is practically constant in time. This recovery towards $G_{22}(t)=1$ corresponds to the motional narrowing of an NMR line and

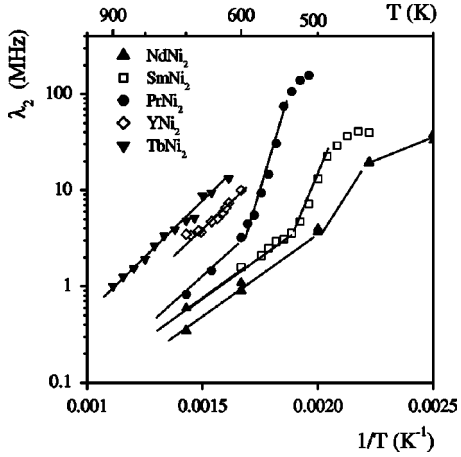

FIG. 7. The relaxation parameter λ_2 of some ^{111}Cd:RNi$_2$ compounds at $T>450$ K.

implies a vanishing time average of the interaction and thus a cubic symmetry of the probe site in the fast-fluctuation limit. The relaxation parameters λ_2 were extracted from the spectra of $PrNi_2$ and $NdNi_2$ between 400 K and 600 K using Eq. (3) with $\Gamma_{22}(t)=1$. The values obtained with the assumption of a single fraction are collected in Fig. 7. In the case of $GdNi_2$ (Fig. 2) and $SmNi_2$ the evidence for a dynamic QI at 400 K is less unambiguous. These spectra can be equally well described by a broad static QI distribution centered at $\nu_q \approx 10$ MHz. At about 500 K, however, a reversible recovery to a constant unperturbed anisotropy sets in also in these compounds and the spectra are well reproduced by a single relaxation parameter λ_2 [Eq. (3)] with $\Gamma_{22}(t)=1$.

For all members of the $R=$Pr, Nd, Sm, Gd group several different compounds of identical composition (1:2 and 0.95:2) were studied. While in $PrNi_2$, $NdNi_2$, and $SmNi_2$ the fraction of probes subject to the QI systematically reached 100% at low temperatures, some samples of $GdNi_2$ presented a superposition of the quadrupole-modulated component and the slowly decaying cubic component down to 100 K, independent of the stoichiometry ratio (1:2 or 0.95:2). In $GdN_{1.05}$ the QI-modulated fraction appeared only after annealing at 1273 K for 8 h. The relative intensity of the QI-modulated component in $GdNi_2$ compounds with the same nominal composition and thermal history was found to vary between 40% and 100%. A relation between the relative intensity and source preparation parameters (e.g., annealing) could not be established.

Some samples of YNi_2 also presented the axially symmetric QI systematically found in the light RNi_2. The relative intensity of this component never reached 100% as in the light RNi_2. In other samples of YNi_2, which were prepared by an apparently identical procedure, the QI did not appear, neither for 1:2 nor 0.95:2 stoichiometry ratios. All samples, however, showed evidence for a fluctuating QI at temperatures $T>500$ K in the form of a reversible recovery of the unperturbed pattern.

B. Heavy RNi$_2$: R=Tb, Dy, Ho, Er, and Sc

Figure 8 illustrates the type of PAC spectrum observed in the second group of the RNi$_2$ series with $R=$Tb, Dy, Ho, and Er using $Tb_{0.98}Ni_2$ as an example. In the magnetically ordered phase one finds a perturbation by a pure magnetic interaction with frequency $\nu_M = g\mu_N B_{hf}/h = 7.3(1)$ MHz at 4.2 K (g represents the nuclear g factor, μ_N the nuclear magneton and $\mathbf{B}_{hf}$ the magnetic hyperfine field). There is no periodic modulation by a QI in the paramagnetic phase $T>T_C$. Instead, the anisotropy decreases monotonically with time, which can be described by a static distribution of weak QI's ($\nu_q \approx 5-10$ MHz). Between 100 K and 500 K, the spectra change very little with temperature. Above 500 K, however, one again observes the reversible recovery towards an unperturbed spectrum, indicating the presence of a rapidly fluctuating QI. The corresponding relaxation parameter λ_2 is shown in Fig. 7. The perturbations—both by the static QI distribution at low and by the dynamic QI's at higher temperatures—become weaker as one moves towards the end of the RNi$_2$ series. In $ErNi_2$ the angular correlation is practically unperturbed at all temperatures $100\ \text{K} \leqslant T \leqslant 700$ K.

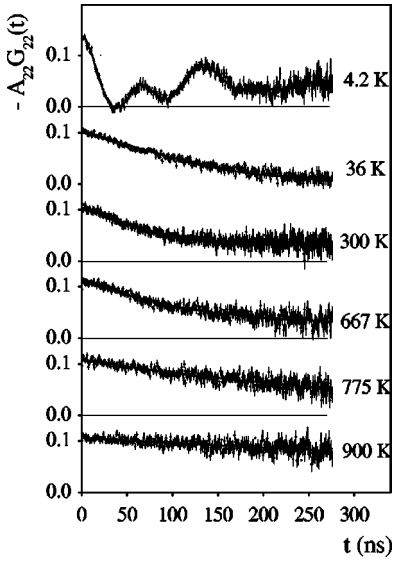

FIG. 8. PAC spectra of ^{111}Cd in $Tb_{0.98}Ni_2$ between 4.2 K and 900 K.

The ^{111}Cd PAC spectrum of $Sc_{0.95}Ni_2$ was measured between 10 K and 1200 K. In spite of the considerable concentration of vacancies in the R sublattice, we observed neither a static QI at low temperatures nor an indication of a dynamic QI at high temperatures. At all temperatures the spectra reflect a static QI distribution with the parameters $\nu_q \approx 10$ MHz, $\eta \approx 0.4$, $\delta \approx 0.8$. $ScNi_2$ and $ScNi_{1.97}$ also presented a static, slightly weaker QI distribution at all temperatures.

C. $Sm_{1-x}In_xNi_2$ and $Pr_{1-x}In_xNi_2$: $x=0.01$ and 0.03

In samples of $PrNi_2$ and $SmNi_2$ doped with radioactive ^{111}In (concentration $\geqslant 10^{-8}$) the QI-modulated fraction systematically reaches 100% at low temperatures. The addition of a sizable concentration of stable indium affects the relative intensity of the QI-modulated component and its relaxation parameter λ_2 at intermediate temperatures. Figure 9

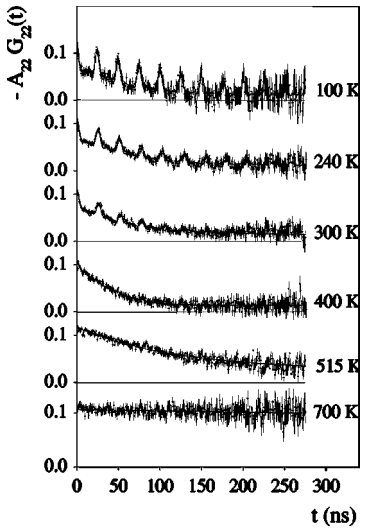

FIG. 9. PAC spectra of ^{111}Cd in $SmNi_2$ doped with 3 at.% of stable indium.

shows PAC spectra of a sample of $SmNi_2$ doped with 3 at.% of stable indium. At 100 K one observes a superposition of the cubic and the QI-modulated component. The temperature dependence of the relative amplitude of the QI-modulated component and of the relaxation parameter λ_2 for indium concentrations of 1% and 3%, respectively, are given in Figs. 10 and 11. Similar results, i.e., reduction of the QI-modulated fraction and the relaxation parameter, were obtained for $Pr_{1-x}In_xNi_2$. At high temperatures $T>500$ K one finds again the reversible evolution towards an unperturbed pattern, indicating the presence of rapidly fluctuating QI's.

D. Gd_2Ni_{17}, $GdNi_5$, $GdNi_3$, and GdNi

The intermetallic compounds Gd_2Ni_{17}, $GdNi_5$, $GdNi_3$, and GdNi show spontaneous magnetic order below Curie temperatures of T_C=196, 29, 115, and 66 K, respectively. We have investigated the hyperfine interactions in both the ferromagnetic and the paramagnetic phase. The combined interaction of the ferromagnetic phase will be discussed in a separate paper. In the context of the present work only the QI in the paramagnetic phase is of interest, which can be extracted from the ^{111}Cd PAC spectra shown in Fig. 12. At $T>T_C$ the spectra of Gd_2Ni_{17} and $GdNi_5$ can be reproduced by a single fraction of probe nuclei, subject to an axially symmetric QI with frequencies ν_q=104 and 109 MHz, respectively, at room temperature. The result for $GdNi_5$ agrees with that of a previous study of ^{111}Cd:$SmNi_5$ (Ref. 19), where it is shown that ^{111}In preferentially occupies the R site of RNi_5. The spectrum of $GdNi_3$ contains two components (intensity ratio ~3:1) with axial symmetry (η=0) and frequencies ν_q=34 and 46 MHz, respectively. The spectrum of GdNi reflects a broad distribution ($\delta\approx0.25$) of QIs centered at $\nu_q\approx20$ MHz, $\eta\approx0.5$.

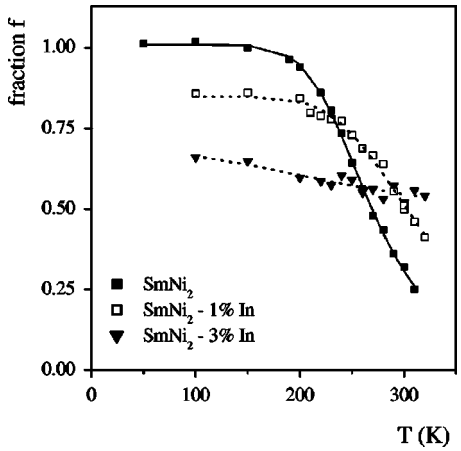

FIG. 10. The temperature dependence of the fraction of ^{111}Cd probe nuclei subject an axially symmetric QI in $SmNi_2$ at different concentrations of stable indium.

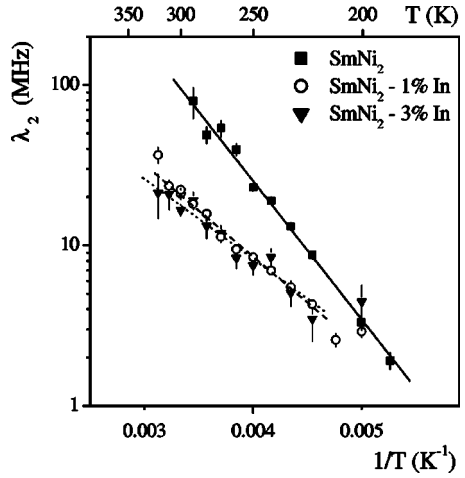

FIG. 11. The relaxation parameter λ_2 of $SmNi_2$ between 200 K and 300 K at different concentrations of stable indium.

IV. DISCUSSION

At $T>500$ K the environment of ^{111}In/^{111}Cd in RNi_2 has cubic symmetry, as indicated by the absence of a QI, which shows that the probes reside on the cubic R site, just as in

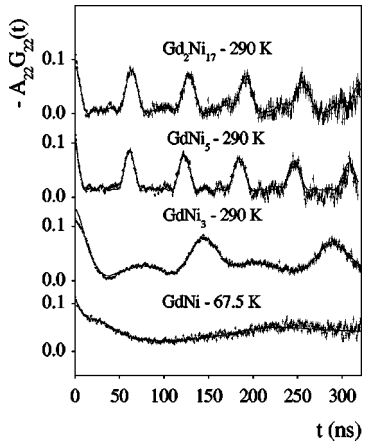

FIG. 12. PAC spectra of ^{111}Cd in the paramagnetic phases of Gd_2Ni_{17}, $GdNi_5$, $GdNi_3$, and GdNi.

analogous $R\mathrm{Co}_2$.[1] The migration of the probes to the noncubic Ni site at $T<300$ K can be excluded because the quadrupole frequencies of ^{111}Cd on the noncubic sites of the very similar $C15$ compounds $R\mathrm{Al}_2$ (Refs. 20 and 21) and HfV_2 (Ref. 22) are a factor of 5 smaller than the frequency observed in $R\mathrm{Ni}_2$. Furthermore, the comparison of the $^{111}\mathrm{Cd}$:$R\mathrm{Ni}_2$ quadrupole frequency $\nu_q=265-275$ MHz with that observed in the other intermetallic compounds of the Gd-Ni system ($\nu_q\leqslant 110$ MHz; see Sec. III D) excludes impurity phases as an explanation of the QI observed at $T<300$ K.

The QI detected in some $R\mathrm{Ni}_2$ at $T<300$ K is not observed in $R\mathrm{Co}_2$. The main crystallographic difference between these two series is the structural instability of $R\mathrm{Ni}_2$, which results in a large concentration of R vacancies. The comparison between $R\mathrm{Co}_2$ and $R\mathrm{Ni}_2$ therefore suggests a relation between the QI and the large number of R vacancies in $R\mathrm{Ni}_2$.

A. Quadrupole interactions expected on the R sites of $R\mathrm{Ni}_2$ with a static superstructure of ordered vacancies

A nearest-neighbor vacancy breaks the symmetry of a cubic site and produces an axially symmetric EFG. The $F\bar{4}3m$ unit cell of $R\mathrm{Ni}_2$ with a superstructure of ordered vacancies on sites $4a$ contains three different R sites. There are 32 R atoms with one nearest-neighbor vacancy in the [111] direction (at distance $0.217a$ in the nonrelaxed structure, where a is the lattice parameter of the superstructure), which produces an axially symmetric EFG $V_{zz}(A)$. 24 R atoms are in the center of two vacancies in the [110] direction (distance $0.354a$), producing an axially symmetric $V_{zz}(B)$. The 4 R sites in the center of 6 vacancies in the [100] directions (distance $0.5a$) have cubic symmetry and zero EFG. For $^{111}\mathrm{In}/^{111}\mathrm{Cd}$ statistically occupying the available R sites in the superstructure with zero occupancy of site $4a$, the PAC spectrum should therefore contain three components with relative intensities of 0.533, 0.4, and 0.067, respectively, the first two perturbed by a QI, the last one unperturbed.

The ratio of QI's of these configurations can be estimated in a point-charge model, assuming that the EFG produced by a vacancy decreases with the third power of the probe-vacancy distance. Using the value of $0.165a$ determined by Latroche *et al.*[6] for the $4a$-$16e$ distance in $R_{1-x}\mathrm{Ni}_2$ ($x=0.06$) and otherwise the nonrelaxed $C15$ distances, one expects a ratio $V_{zz}(B)/V_{zz}(A)\approx 0.2$. If one attributes the QI ($\nu_q=265$ MHz) observed in $R\mathrm{Ni}_2$ with $R=\mathrm{Pr,Nd,Sm,Gd}$ to a vacancy at $0.165a$ [$V_{zz}(A)$], the second configuration would produce a quadrupole frequency of the order of $\nu_q\approx 50$ MHz, which should still be detectable in the ^{111}Cd time window of 300 ns. If the observed QI is related to the superstructure, both components should appear in the PAC spectra at all temperatures below the order-disorder temperature in all $R\mathrm{Ni}_2$, also $R=$Tb, Dy, Ho, and Er. The intensity of these components depends on the occupancy N of site $4a$, which strongly increases from the light to the heavy $R\mathrm{Ni}_2$ ($N=0.12$ and 1 for PrNi_2 and LuNi_2, respectively[6]). A value of $N\approx 1$ might explain the absence of a QI in ErNi_2 but not for TbNi_2 where the existence of the superstructure is well established by x-ray diffraction.[9] For TbNi_2 $4a$ occupancies $N=0.75$ have been reported.[9] This would correspond to a minimum intensity of the 265 MHz component of 12.5% that is easily detectable in a ^{111}Cd PAC spectrum. Our experimental observations of (i) one cubic and one QI-modulated component for $R=\mathrm{Pr,Nd,Sm,Gd}$, (ii) the temperature dependence of the QI-modulated fraction, reaching 100% at $T<150$ K, (iii) the fluctuations of the QI at intermediate temperatures, and (iv) the absence of the QI for $T=$Tb, Dy, Ho, and Er therefore cannot be explained by a static superstructure of ordered vacancies.

B. Evidence for vacancy trapping by ^{111}In in $R\mathrm{Ni}_2$ at 100 K$\leqslant T\leqslant$300 K

PAC studies in pure metals have established that the probe $^{111}\mathrm{In}/^{111}\mathrm{Cd}$ may act as a trap for vacancies.[23] A monovacancy trapped by $^{111}\mathrm{In}/^{111}\mathrm{Cd}$ on a cubic site produces a sharp, axially symmetric QI with frequencies of the order of $\nu_q\approx 100-200$ MHz. The vacancy concentration of normal metals at room temperature is of the order of a few ppm, too small for an observable PAC signal. In these studies, larger vacancy concentrations are therefore produced at low temperatures by, e.g., cold working or ion bombardment, and their trapping and detrapping are studied by PAC measurements at low temperatures after successive isochronous annealing steps. In the case of $R\mathrm{Ni}_2$ the structural instability leads to a thermal equilibrium vacancy concentration c_V of a few percent, which is much larger than the usual probe concentration c_P of a diffused $^{111}\mathrm{In}/^{111}\mathrm{Cd}$ PAC sample.

With the assumption that $^{111}\mathrm{In}/^{111}\mathrm{Cd}$ constitutes an attractive potential for vacancies with a binding energy E_{PV} (probe vacancy), two fractions of probe nuclei are expected at intermediate temperatures. The probes with a nearest-neighbor vacancy are subject to an axially symmetric QI and constitute the "QI-modulated" fraction f; probes on cubic sites without a nearby vacancy are—ideally—unperturbed (in reality, slight structural and chemical imperfections or vacancies at larger distances to the probe may lead to weak quadrupole perturbations) and constitute the "cubic" fraction $(1-f)$. The temperature dependence $f(T)$ resulting from this picture can be calculated by considering two possible vacancy states, separated by the energy E_{PV}. In the ground state, a vacancy has a probe nucleus as nearest neighbor; the excited state corresponds to vacancies surrounded by R atoms only. The degeneracies of the ground and exited states are nc_P and $(1-nc_P)$, respectively, where n is the number of nearest R neighbors of a given R site. In the $C15$ lattice one has $n=4$. The occupation probability of the ground state gives the thermal equilibrium fraction of probe nuclei with a nearest-neighbor vacancy:

$$f(T)=f_0\frac{1}{1+(1/nc_p-1)\exp(-E_{PV}/k_BT)}, \qquad (6)$$

with $f_0=1$ for $c_V\geqslant c_P$ and $f_0=c_V/c_P$ for $c_V<c_P$.

Equation (6) provides an explanation for the experimentally observed temperature dependence of the QI-modulated fractions in Fig. 3. At temperatures $T\ll E_{PV}/k_B$ (k_B is the

Boltzmann constant) all probes have trapped a vacancy, but when the thermal energy exceeds the binding energy at $T \geqslant E_{PV}/k_B$ detrapping sets in and the fraction f of vacancy-decorated probes decreases towards $f = f_0 n c_P$.

In Eq. (6) the binding energy E_{PV} and the probe concentration c_P are strongly correlated and an independent determination of these two parameters requires a strong variation of $f(T)$ in the temperature range investigated. The strongest variation of $f(T)$ is found in the case of $SmNi_2$. A least squares fit of Eq. (6) with free parameters to these data (solid line in Fig. 3) gives a probe-vacancy binding energy of $E_{PV}=0.18(1)$ eV and a probe concentration of $c_P=8\times10^{-5}$. Fixing the probe concentration to $c_P=8\times10^{-6}$ results in a still acceptable fit with a binding energy $E_{PV}=0.23$ eV; smaller probe concentrations, however, are incompatible with the experimental data if a sharp value of E_{PV} is assumed in the analysis.

The probe concentration derived from $f(T)$ thus appears to be in conflict with the value estimated from the γ-ray intensity of the source ($c_P \approx 10^{-8}$). This discrepancy can, however, be resolved by admitting a finite distribution—rather than a unique value—of the probe-vacancy binding energy E_{PV}. For a well defined E_{PV}, the probe concentration c_P determines the sharpness of the transition from $f \approx 1$ to $f \approx 0$ [see Eq. (6): the smaller the probe concentration, the smaller the temperature interval of the transition]. A broad transition region of $\approx$100 K as in the case of $SmNi_2$ therefore suggests a large probe concentration. A distribution of E_{PV}, however, also broadens the transition and c_P is therefore easily overestimated if a sharp value of E_{PV} is used in the analysis of $f(T)$. In the case of $SmNi_2$ it is sufficient to assume a distribution (Lorentzian or Gaussian) of E_{PV} with a relative width of the order of 10% to reproduce the experimental variation of $f(T)$ with the probe concentration fixed to $c_P=10^{-8}$, the value obtained from the γ-ray intensity.

The difficulties of separating E_{PV} and c_P are even more pronounced in the case of $PrNi_2$, $NdNi_2$, and $GdNi_2$, where the observed variation of $f(T)$ is rather weak. [The reason that $f(T)$ cannot be followed to higher temperatures is the destruction of the QI modulation by the QI fluctuations, which makes a separation of the cubic and the QI-modulated fraction at $T>300$ K impossible]. Fits to the data of $PrNi_2$, $NdNi_2$, and $GdNi_2$ in Fig. 3 may differ in c_P by several orders of magnitude and still be of acceptable quality. A parameter better suited for an unambiguous characterization of $f(T)$—especially in cases where the observed variation is relatively weak—is the temperature at which the fraction has dropped to $f_0/2$:

$$T(f_0/2) = \frac{E_{PV}}{k_B \ln(1/nc_P - 1)}. \tag{7}$$

In the case of a E_{PV} distribution, $T(f_0/2)$ reflects the most probable probe-vacancy binding energy. Table I shows the values of $T(f_0/2)$ obtained for $PrNi_2$, $NdNi_2$, $SmNi_2$, and $GdNi_2$. The values of $T(f_0/2)$ of different samples of $SmNi_2$ and $GdNi_2$ were found to differ up to 20%. Different samples of $PrNi_2$ and $NdNi_2$ showed the same variation of $f(T)$ up to 300 K, but as this variation is rather weak, considerable systematic uncertainties arise even for the parameter $T(f_0/2)$. The data in Table I clearly show a decrease of $T(f_0/2)$ from the light to the heavy R constituents of RNi_2. As the probe concentration c_P can be assumed to be of the same order of magnitude in all samples, the decrease of $T(f_0/2)$ reflects a decrease of the probe-vacancy binding energy E_{PV} from the light to the heavy RNi_2. Such a trend could explain the absence of a QI in the second RNi_2 group with R=Tb, Dy, Ho, and Er. According to Ref. 6, the distance between a vacancy on site 4*a* and the nearest-neighbor (NN) (16*e*) R site is more or less constant between Pr and Gd, but starting at Tb it strongly increases towards the end of the RNi_2 series. Because of a larger probe-vacancy separation, $^{111}In/^{111}Cd$ no longer constitutes vacancy trap so that the QI does not appear in the second RNi_2 group. An increase of the probe-vacancy distance from the light to the heavy RNi_2 is also suggested by the decrease of the quadrupole frequency ν_q(100 K) from $PrNi_2$ to $GdNi_2$ (see Table I).

The ^{111}Cd QI does not appear in $GdNi_2$ when the 245 keV state is populated by the decay of ^{111}Ag. ^{111}In and ^{111}Ag are of similar size and considerably smaller than the R atoms they substitute. The obvious difference in the probe-vacancy interaction energy of these two probe atoms is therefore difficult to explain by size arguments. Possibly the different electronic configurations play a role.

C. Vacancy motion and nuclear spin relaxation at 100 K$\leqslant T \leqslant$300 K

The observation that the QI-modulated fraction increases towards low temperatures implies a migration of vacancies towards the probe nuclei. The potential barrier, which R atoms have to overcome in this migration, can be estimated from the time it takes to establish thermal equilibrium at a given temperature. With the closed-cycle He refrigerator used in our experiments it takes about 1 h to cool a sample from room temperature to 100 K. This time is obviously sufficient to establish thermal equilibrium, since the QI-modulated component saturates at 100%. Assuming a jump frequency of $w=1\ s^{-1}$ at 100 K (4×10^3 jumps in 1 h), one obtains from an upper limit of the barrier height of $E_A \approx 0.25(4)$ eV for atomic vibration frequencies in the range $w_0 \approx 10^{10}-10^{12}\ s^{-1}$.

Evidence for atomic motion in RNi_2 also comes from the nuclear spin relaxation manifest in the attenuations of the QI modulations between 200 K and 300 K. The increase of the relaxation parameter λ_2 with temperature reflects slow fluctuations of the perturbing interaction (see Sec. II B). At 250 K the hopping frequency $w \approx \lambda_2 \approx 10$ MHz (time between jumps $\tau = 1/w \approx 100$ ns) is in fact small compared to the static interaction $\nu_q=265$ MHz.

The ^{111}Cd PAC time window for the observation of nuclear relaxations opens when the decay of ^{111}In populates the intermediate state of the 171–245 keV cascade of ^{111}Cd. In this moment, the decaying ^{111}In may either be decorated by a trapped vacancy and thus belong to the QI-modulated fraction or be part of the cubic fraction with four NN R atoms. Because of the r^{-3} dependence of the EFG, the QI will strongly decrease when nearest-neighbor vacancies of

the probe jump to second-NN positions. In a simplifying picture, we may assume that the EFG is switched off. On the other hand, the EFG is switched on when R atoms of the cubic fraction jump to a vacant site in the second-nearest-neighbor shell. Both processes produce fluctuations of the QI at the ^{111}Cd sites.

The strength of the fluctuating QI can be estimated without exact knowledge of the correlation time from the fact that the maximum of the relaxation parameter λ_2^{max} and the frequency ν_q^f of the fluctuating QI are related by $\lambda_2^{max} \approx 1/2\nu_q^f$ (Refs. 15 and 16). In the present case one has $\lambda_2^{max} \leqslant 100$ MHz (see Fig. 4), so that the dynamic QI ($\nu_q^f \approx 200$ MHz) at intermediate temperatures is very similar to the static QI ($\nu_q = 265-275$ MHz) at low temperatures, which we associate with the EFG produced by a vacancy trapped in a nearest-neighbor position of the probe. After a jump to the second-NN shell of the probe, a vacancy may either jump back to the NN position or move away. In the latter case, the fluctuating QI would become weaker than the static QI at low temperatures. The agreement between ν_q^f and ν_q therefore suggests that the nuclear relaxation observed at 200 K $\leqslant T \leqslant$ 300 K is caused by vacancies jumping forth and back between nearest- and second-nearest-neighbor positions of the probe and implies that not only ^{111}In, but also ^{111}Cd constitutes an attractive potential for vacancies. (Note: The probe swapping position with a NN vacancy cannot account for the observation of a fluctuating QI because neither the magnitude nor the orientation of the EFG would be affected by such an interchange.)

The activation energy E_A for vacancy jumps in the immediate probe environment derived from the temperature dependence of the relaxation parameter $\lambda_2(T)$ at 200 K $\leqslant T \leqslant$ 300 K is similar to the barrier height estimated from the thermal equilibrium time constant (see above). Our data indicate that the activation energy depends in some way on the details of the sample preparation, because the values of E_A in several samples of the same compound may differ considerably (see Fig. 6). The values derived from all measurements of $\lambda_2(T)$ cover a range of 0.1 eV $\leqslant E_A \leqslant$ 0.23 eV. These activation energies are surprisingly small, comparable to the activation energies of fast interstitial diffusion of very small atoms in metals (e.g., for H in Fe, $E_A \approx 0.13$ eV). It is because of these very small activation energies that the observations reported here could be made at all. With $E_A = 0.5$ eV it would literally take years for the QI-modulated fraction to reach 100% at 100 K and the time between jumps at 250 K would be somewhere between 10^{-2} s and 10 s (depending on the atomic vibration frequency), which is by far too long to be detected in a 500 ns PAC window.

In the slow relaxation regime $T < 300$ K the relaxation parameter λ_2 is determined by the jump frequency w: $\lambda_2 = \alpha w$. The preexponential factor λ_2^0 in the relation is therefore a direct measure of the atomic vibration frequency w_0. It is interesting to see that the values of λ_2^0 derived from the experimental $\lambda_2(T)$ dependence correlate with the activation energy E_A (see Fig. 6), suggesting that the lower the barrier height the slower the atomic vibration.

The unusually small activation energy and the puzzling correlation between the activation energy and the trial frequency might be related to the exceptionally high equilibrium concentration of vacancies in $R_{1-x}Ni_2$. In view of these observations, an investigation of the diffusion processes in $R_{1-x}Ni_2$ by classical techniques would be of great interest.

D. Vacancy-induced nuclear spin relaxation at $T > 500$ K

At temperatures $T > 500$ K, the relaxation parameter decreases with increasing temperature, indicating rapid fluctuations of the perturbing interaction. The temperature dependence of $\lambda_2(T)$ in the fast-fluctuation regime, however, does not follow a simple Arrhenius behavior. In most cases, one finds a small temperature interval with a very strong decrease of λ_2, followed by a weaker variation at higher temperatures. In $PrNi_2$, e.g., the relaxation parameter drops by a factor of 10 between 550 K and 600 K (see Fig 7), which is clearly visible in Fig. 1 as a rapid recovery of the PAC towards a constant anisotropy. For fast fluctuations the relaxation depends on the strength of the fluctuation interaction (ν_q^f) and the correlation time τ_C (time between jumps): $\lambda_2 \propto (\nu_q^f)^2 \tau_C$ [see Eq. (4)]. If attributed to the correlation time alone, the strong decrease of λ_2 would correspond to an activation energy of $E_A \approx 1.6$ eV. It appears rather implausible that the activation energies in the slow- and the fast-fluctuation regimes should differ by a factor of 5. More likely, the strong decrease of λ_2 reflects a decrease of ν_q^f, which is expected when the thermal energy exceeds the ^{111}Cd-vacancy binding energy and the trapped vacancies may jump away from the probe nuclei. Although the high-temperature PAC spectra clearly show the presence of a rapidly fluctuating QI, an unambiguous analysis, in particular, the separation of the dynamic QI from eventual contributions by static QI distributions, is very difficult. We therefore abstain from a quantitative discussion of $\lambda_2(T)$ for $T > 500$ K.

The nuclear spin relaxation at high temperatures is not restricted to those RNi_2 which show a static QI at low temperatures. The spectra of ^{111}Cd:$Tb_{0.98}Ni_2$ (Fig. 8) present clear evidence of a spin relaxation at $T > 650$ K. Although vacancies are not trapped in $Tb_{0.98}Ni_2$, their rapid motion at large distances to the probe leads to fast fluctuations of weak QI's, which explains the recovery of the unperturbed angular correlation at high temperatures. Such a motional narrowing is absent in $ErNi_2$, probably because of the small vacancy concentration at the end of the RNi_2 series.[6] The absence of a dynamic QI at high temperatures in $Sc_{0.95}Ni_2$ in spite of a vacancy concentration of 5% indicates that in $Sc_{0.95}Ni_2$ the potential barrier to be overcome by hopping vacancies is much larger than in $R_{1-x}Ni_2$, which might be due to the close packing of the atoms in $ScNi_2$.

E. Estimate of the concentration of migrating vacancies

The PAC observations, in particular the temperature dependence of the QI-modulated fraction (see Fig. 3) and of the nuclear spin relaxation (see Fig. 4) leave little doubt that atomic motion occurs in RNi_2 at temperatures $T < 300$ K on a time scale of 10^{-7} s. On the other hand, the temperature dependence of the superstructure intensity in the x-ray diffraction spectra of $R_{1-x}Ni_2$ (see Fig. 5) suggests a stable vacancy superstructure at $T \leqslant 350$ K.

The difference in the pictures suggested by PAC and x-ray diffraction might have a simple explanation: The PAC detects only the vacancies trapped at the radioactive probes. As their concentration is very small, one cannot *a priori* exclude that only a minute fraction of the vacancies participates in the migration, while the rest is bound in the superstructure. This leads to the important question of how many vacancies are involved in the observed dynamic effects, which is answered by the measurements described in Sec. III C: In order to reduce the fraction of QI-modulated probes at $T<100$ K below 100% [$f_0=c_V/c_P<1$ in Eq. (6)], one has to add stable indium to a concentration $c_P=10^{-2}$ (see Fig. 10). As the vacancies cannot distinguish stable from radioactive indium, this observation means that the concentration c_V of migrating vacancies must be of the order of a few percent and implies that practically all vacancies of $R\mathrm{Ni}_2$ are highly mobile below the order-disorder temperature.

The apparently resulting conflict between the PAC evidence of highly mobile vacancies and the x-ray diffraction pattern of an ordered vacancy superstructure at $T<300$ K might be a consequence of the different time scales involved in the two techniques. While the ^{111}Cd PAC time window is of the order of 10^{-7} s, the integration time of usual x-ray diffraction is about 10 orders of magnitude longer and the x-ray pattern reflects the time-averaged symmetry of the compound. To resolve the apparent conflict between the PAC and the x-ray observations, it would therefore be sufficient to postulate that on the average the residence time of the rapidly moving vacancies on site 4*a* is somewhat longer than on the other *R* sites of $R\mathrm{Ni}_2$.

V. SUMMARY

Rare-earth-deficient $R_{1-x}\mathrm{Ni}_2$ Laves phases, which reportedly crystallize in a *C*15 superstructure with ordered *R* vacancies, have been investigated by PAC measurements of electric quadrupole interactions at the site of probe nucleus ^{111}Cd. Although ^{111}Cd resides on the cubic *R* site, a strong axially symmetric QI with frequencies $\nu_q\approx 265-275$ MHz has been found in the paramagnetic phases of $R_{1-x}\mathrm{Ni}_2$ for $R=\mathrm{Pr,Nd,Sm,Gd}$. This interaction is not observed for the heavy *R* constituents $R=\mathrm{Tb,Dy,Ho,Er}$. The fraction of probe nuclei subject to the QI in $R_{1-x}\mathrm{Ni}_2$, $R=\mathrm{Pr,Nd,Sm,Gd}$, reaches 100% at low temperatures and vanishes at $T>300$ K and 500 K for $R=\mathrm{Sm,Gd}$ and $R=\mathrm{Pr,Nd}$, respectively. At $T=100$ K the QI is static within the PAC time window, but at $T\geqslant 200$ K fluctuations with correlation times $\tau_C<10^{-6}$ s have been detected. These observations can be explained consistently by two assumptions: (i) the mother isotope ^{111}In of the PAC probe ^{111}Cd constitutes an attractive potential for vacancies and (ii) the *R* vacancies in $R_{1-x}\mathrm{Ni}_2$ are highly mobile at temperatures $T<300$ K, which is incompatible with a static vacancy structure. The probe-vacancy binding energy can be estimated from the temperature dependence of the fraction of probe nuclei decorated with a vacancy. The PAC measurements indicate a decrease of this energy from the light to the heavy *R* constituents of $R_{1-x}\mathrm{Ni}_2$, which may explain the absence of the QI for $R=\mathrm{Tb,Dy,Ho,Er}$. For $R=\mathrm{Pr,Nd,Sm,Gd}$ the binding energy is in the range 0.15–0.40 eV. The activation energy E_A for jumps of *R* atoms near the probe derived from the temperature dependence of the nuclear relaxation at $200\ \mathrm{K}\leqslant T\leqslant 300$ K is surprisingly small. The values observed in different samples cover a range of $0.1\ \mathrm{eV}\leqslant E_A\leqslant 0.23$ eV. The trial frequency w_0 of these jumps appears to be correlated to the activation energy. The relaxation data indicate an increase from $w_0\approx 10^9\ \mathrm{s}^{-1}$ at $E_A=0.1$ eV to $w_0\approx 10^{12}\ \mathrm{s}^{-1}$ at $E_A=0.23$ eV. At high temperatures $T>500$ K nuclear spin relaxation related to vacancy hopping is observed in nearly all $R_{1-x}\mathrm{Ni}_2$, also in most of those that show no static QI at low temperatures.

ACKNOWLEDGMENTS

Two of the authors would like to express their gratitude for financial support, P.P. from "Deutscher Akademischer Austauschdienst" (DAAD) and A.L. from the Austrian Academy of Sciences (APART 10739) and the Austrian Science Fund FWF (P14932).

*Author to whom correspondence should be addressed. Electronic address: forker@iskp.uni-bonn.de

[1] P. de la Presa, S. Müller, A. F. Pasquevich, and M. Forker, J. Phys.: Condens. Matter **12**, 3423 (2000).
[2] M. Forker, S. Müller, P. de la Presa, and A. F. Pasquevich, Phys. Rev. B **68**, 014409 (2003).
[3] E. Gratz and A. S. Markosyan, J. Phys.: Condens. Matter **3**, R385 (2001).
[4] S. Müller, P. de la Presa, and M. Forker, Hyperfine Interact. **133**, 59 (2001).
[5] M. Latroche, V. Paul-Boncour, A. Percheron, and J. C. Achard, J. Less-Common Met. **161**, L27 (1990).
[6] M. Latroche, V. Paul-Boncour, and A. Percheron, Z. Phys. Chem. (Munich) **179**, 621 (1993).
[7] E. Gratz, A. Kottar, A. Lindbaum, M. Mantler, M. Latroche, V. Paul-Boncour, M. Acet, Cl. Barner, W. B. Holzapfel, V. Pacheco, and K. Yvon, J. Phys.: Condens. Matter **8**, 8351 (1996).
[8] A. Lindbaum, J. Hafner, E. Gratz, and S. Heathman, J. Phys.: Condens. Matter **10**, 8351 (1998).
[9] A. Lindbaum, E. Gratz, and S. Heathman, Phys. Rev. B **65**, 134114 (2002).
[10] A. Lindbaum, J. Hafner, and E. Gratz, J. Phys.: Condens. Matter **11**, 1177 (1999).
[11] M. Forker, W. Herz, U. Hütten, M. Müller, R. Müßeler, J. Schmidberger, D. Simon, A. Weingarten, and S. C. Bedi, Nucl. Instrum. Methods Phys. Res. A **327**, 456 (1993).
[12] H. Frauenfelder and R. M. Steffen, in *Perturbed Angular Correlations*, edited by K. Karlsson, E. Matthias, and K. Siegbahn (North-Holland, Amsterdam, 1963).

[13] M. Blume, Phys. Rev. **174**, 351 (1968).
[14] K. H. Winkler and E. Gerdau, Z. Phys. **262**, 363 (1973).
[15] A. Boudry and P. Boyer, Hyperfine Interact. **25**, 803 (1987).
[16] M. Forker, W. Herz, and D. Simon, Nucl. Instrum. Methods Phys. Res. A **337**, 534 (1993).
[17] A. Abragam and R. V. Pound, Phys. Rev. **92**, 943 (1953).
[18] M. Forker, L. Freise, and D. Simon, Z. Naturforsch. Teil A **41A**, 99 (1986).
[19] S. H. Devare, R. G. Pillay, S. K. Malik, S. K. Ghar, and H. G. Devare, Phys. Lett. **79A**, 237 (1980).
[20] R. G. Pilley, K. Raghunathan, P. N. Tandon, S. H. Devare, and H. G. Devare, Phys. Lett. **91A**, 193 (1982).
[21] M. Forker, P. de la Presa, M. Olzon-Dionysio, and S. Dionysio de Souza, J. Magn. Magn. Mater. **226-230**, 1156 (2001).
[22] M. Forker, W. Herz, D. Simon, and S. C. Bedi, Phys. Rev. B **51**, 15994 (1995).
[23] E. Recknagel, G. Schatz, and Th Eichert, in *Hyperfine Interactions of Radiactive Nuclei* Topics in Current Physics, No. 31, edited by J. Christiansen (Springer, Berlin, 1983).